
Minimal spanning tree algorithm for γ -ray source detection in sparse photon images: cluster parameters and selection strategies.

R. Campana • E. Bernieri • E. Massaro •
F. Tinebra • G. Tosti

Abstract The minimal spanning tree (MST) algorithm is a graph-theoretical cluster-finding method. We previously applied it to γ -ray bidimensional images, showing that it is quite sensitive in finding faint sources. Possible sources are associated with the regions where the photon arrival directions clusterize. MST selects clusters starting from a particular “tree” connecting all the point of the image and performing a cut based on the angular distance between photons, with a number of events higher than a given threshold. In this paper, we show how a further filtering, based on some parameters linked to the cluster properties, can be applied to reduce spurious detections. We find that the most efficient parameter for this secondary selection is the *magnitude* M of a cluster, defined as the product of its number of events by its *clustering degree*. We test the sensitivity of the method by means of simulated and real *Fermi*-Large Area Telescope (LAT) fields. Our results show that \sqrt{M} is strongly correlated with other statistical significance parameters, derived from a wavelet based algorithm and maximum likelihood (ML) analysis, and that it can be used as a good estimator of statistical significance of MST detections. We apply the method to a 2-year LAT image at energies higher than 3 GeV, and

we show the presence of new clusters, likely associated with BL Lac objects.

Keywords Gamma rays: general – Methods: data analysis

1 Introduction

Telescopes for medium and high energy γ -ray astronomy usually detect individual photons by means of the electron-positron pairs generated through the instrument: from their trajectories it is possible to reconstruct the original direction of the photon, with an uncertainty that decreases from a few degrees below 100 MeV to a few tenths of a degree above 1 GeV. The resulting product is an image where each photon is associated with a direction in the sky: discrete sources correspond thus to small size regions with a localized concentration of photons higher than in the surroundings. When the size of this region and the photon spatial distribution are consistent with the instrumental point spread function (PSF) the source is considered as point-like, otherwise it can be an extended feature or an unresolved group of close sources. Various algorithms are applied to the detection of point-like or extended sources: among them, Maximum Likelihood (Mattox et al. 1996), Multi-Resolution Filter (Starck et al. 1995), Multi-Scale Variance Stabilizing Transform (Schmitt et al. 2012), Optimal Filter (Tegmark and de Oliveira-Costa 1998), Aperture Photometry (Harnden et al. 1984), Wavelet Transform analysis (Damiani et al. 1997), etc. Some of these (like Wavelet Transform or Optimal Filter) are based on deconvolution techniques of the PSF, while other methods search for clusters in the arrival directions of photon that, if statistically significant, are considered an indication for the presence of a source.

R. Campana

INAF/IAPS, Rome and INAF/IASF-Bologna, Bologna, Italy.

E. Bernieri

INFN/LNF and Department of Physics, University of Roma Tre, Rome, Italy.

E. Massaro

Department of Physics, University of Rome “La Sapienza”, Rome, Italy.

F. Tinebra

Department of Physics, University of Rome “La Sapienza”, Rome, Italy.

G. Tosti

Department of Physics, University of Perugia, Perugia, Italy.

In previous papers (Campana et al. 2008; Massaro et al. 2009b), we described the *minimal spanning tree* (MST) algorithm for the search of photon clusters to be associated with γ -ray source candidates. This technique has its root in graph theory, and highlights the *topometric* pattern of “connectedness” of the detected photons.

In the field of high energy astrophysics, source detection with MST was first proposed by Di Gesù and Sacco (1983) for the COS-B mission. Further developments were made by Di Gesù and Maccarone (1986); De Biase et al. (1986); Maccarone et al. (1986); Buccheri et al. (1988), all of these before the observations of *COMP-TON/GRO-EGRET* and *Fermi*-Large Area Telescope (LAT). In other astronomical contexts, MST-based methods were applied to the goal of finding galaxy clusters, both in 2 and 3-dimensional surveys and simulations (Barrow et al. 1985; Bhavsar and Ling 1988b,a; Plionis et al. 1992; Krzewina and Saslaw 1996). These authors also show the capabilities of the MST as a filament-finding algorithm. More recently, MST has been used for studying the clustering of stars by Koenig et al. (2008) and Schmeja (2011), who applied some parameters proposed by us (Massaro et al. 2009b) for the cluster selection. The advantage of MST, and of other cluster-finding algorithms such as DBSCAN (Tramacere and Vecchio 2013), is the capability to quickly find potential γ -ray sources by examining only the incoming directions of the photons, regardless of their energy distribution. This can be useful to find transient sources, that can only be observed by performing a periodic and systematic data analysis over time intervals of weeks or months, or to produce lists of candidate sources that can be further analysed with other well-recognized statistical methods, such as maximum likelihood (ML).

Despite the fact that MST is not the optimal cluster-finding algorithm from the point of view of computational speed, it has the great advantage of providing some useful parameters, that are evaluated over the entire region under consideration, and are relevant for the selection of interesting clusters, as we will show in this paper. We already applied the MST algorithm for detecting clusters of photons in the γ -ray sky in order to obtain lists of candidate sources for the 1FGL and 2FGL *Fermi*-LAT catalogues (Abdo et al. 2010; Nolan et al. 2012). In this application of MST to LAT data, however, we faced some challenges, such as the assessment of the optimal detection threshold, the accuracy of sources’ coordinates — relevant for a safe identification of possible counterparts of γ -ray sources — and the detection significance.

We are mainly interested in the detection of clusters having a rather small number of photons, typically less than 10, that could be associated with faint

γ -ray sources. This problem is important in γ -ray astrophysics because many sources, particularly blazars, are highly variable with short duty-cycles, and therefore their detection becomes harder with long observations when the integrated background level increases with time and the source signal may fade. In this paper we present some new methods to improve the capabilities of MST for detecting γ -ray source candidates, based on our experience in the analysis of LAT data. We will show that it is possible to establish some rather simple criteria for the selection of the best source candidates, applying the method to simulated and real *Fermi*-LAT sky test fields. We also compare MST results with those obtained applying the Perugia Wavelet (PGW) transform code (Ciprini et al. 2007). Based on this comparison, we will show that it is possible to obtain a satisfactory estimate of the statistical detection significance, considering only one of the “cluster parameters” we introduce.

This paper is organised as follows. In Section 2 a brief review of the MST method is given, and in Section 3 we discuss some problems arising in the application of the MST to γ -ray data. In Section 4 we present a way to improve the source localization accuracy, in Section 5 we introduce some parameters able to discriminate between good and spurious sources, and in Section 6 we show the results of the method on simulated fields. In Section 7 we compare MST and PGW results, in Section 8 we analyze the true 2-year LAT field and in Section 9 we discuss the properties of new clusters detected by MST in a real 2-year *Fermi*-LAT field and their possible counterparts. Finally, in Section 10 we draw our conclusions.

2 The MST algorithm for cluster search

In the following we outline the major steps in MST source detection; for a more complete description of the method and of its statistical properties see Campana et al. (2008).

Once having a set of N spatially distributed *nodes*, one can compute the set $\{\lambda_i > 0\}$ of weighted *edges* connecting them: the MST is the tree satisfying the condition $\min[\sum_i \lambda_i]$ (Zahn 1971). For a set of points in a Cartesian frame the edges are the lines joining the nodes, weighted by their length; for a set of points over a spherical surface, like in astronomical imaging, the weights are the angular distances. Several algorithms for the MST computation are available. One widely used was developed by Prim (1957): it starts from an arbitrary selected node, finds the nearest neighbour and connects them with an edge, which is thus the first MST

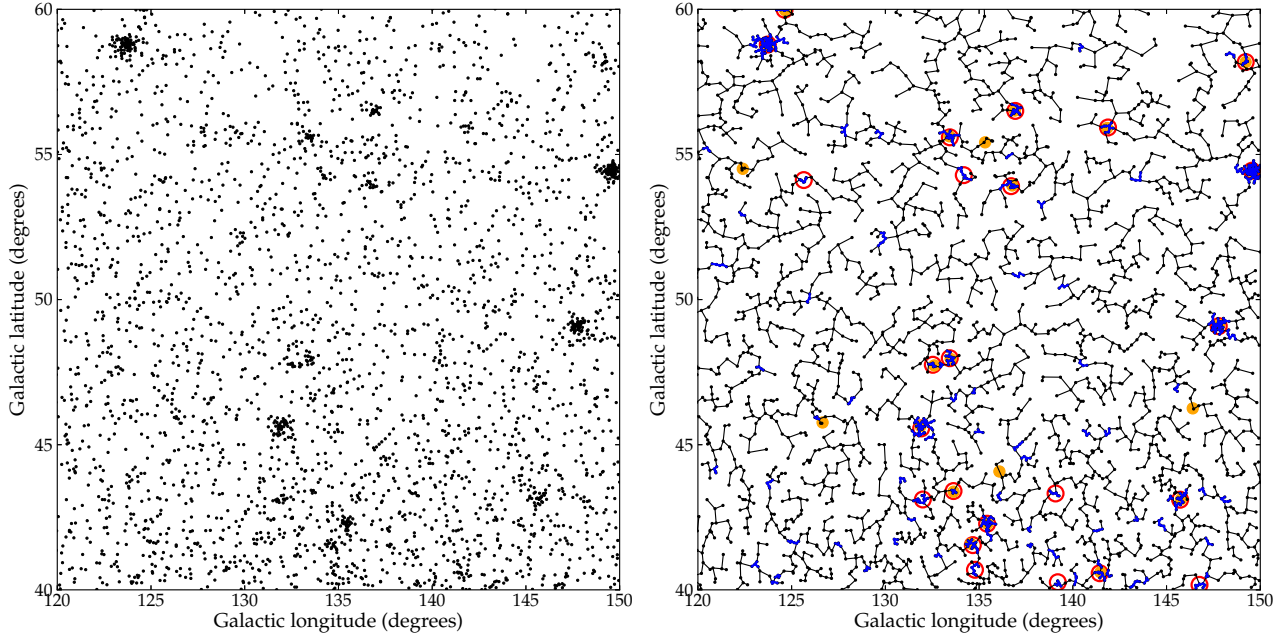


Fig. 1 A example of MST source detection in a LAT field. Left panel: A region ($30^\circ \times 20^\circ$) of the 2-years LAT sky at energies >3 GeV centered at $l = 135^\circ$, $b = 50^\circ$. Right panel: the MST between the photons and the clusters (in blue) found applying the selection criteria $\Lambda_{\text{cut}} = 0.7 \Lambda_m$ and $N_{\text{cut}} = 3$. Red circles mark the candidate γ -ray sources after the secondary selection on M (see Sect. 5); yellow circles mark the positions of sources in the LAT 2FGL catalog, that includes also sources detected only at lower energies.

edge. Then it finds the point that is the nearest to any point that is already connected in the tree. After $N - 1$ iterations, the complete MST is found. Faster and computationally optimized codes can be found using other theoretical properties of the MST, like being a subset of the Delaunay triangulation of the graph. In particular, we used a fast code for the MST computation that uses the freely available BOOST¹ and CGAL² libraries.

To extract *only* the photons that cluster in regions with a density higher than the mean one in the field, i.e. the candidate sources, the following operations are performed:

- **Separation:** remove all the edges having a length $\lambda > \Lambda_{\text{cut}}$, the *separation value*, that can be defined either in absolute units or in units of the mean edge length in the MST: $\Lambda_m = (\sum_i \lambda_i) / (N - 1)$; we thus obtain a set of disconnected sub-trees.
- **Elimination:** remove all the sub-trees having a number of nodes $n \leq N_{\text{cut}}$. We thus remove small random clusters of photons, leaving only the clusters having a size greater than the selected lower limit.

After the application of these two filters, the remaining set of sub-trees $\{S_k\}$ provides a list of clusters, which in our case are candidate γ -ray sources.

When applied to the γ -ray sky, we start with a LAT photon list that contains the arrival directions of all accepted events, time, energy, and other useful parameters. In a selected region, typically large enough to cover at least tens of square degrees, we consider the photon arrival directions as the nodes in the bi-dimensional graph, the edge weight being the angular distance between them, and compute the MST. An example of a sky image, at energies higher than 3 GeV, is shown in the left panel of Fig. 1, while the MST that connects the event positions is presented in the right panel, where the residual subtrees after the two aforementioned operations are marked in blue.

Campana et al. (2008) studied the distribution of edge lengths in MST (Barrow et al. 1985) for random Poissonian fields³ and found that it is well fitted by a Rayleigh distribution modified by a Fermi-Dirac factor. When clusters are present the distribution changes and becomes more asymmetric, with an excess of both short

¹<http://www.boost.org>

²<http://www.cgal.org>

³The formal definition of a spatial Poisson process with uniform density involves the fact that in each closed subregion the number of points follow a Poisson distribution, and the various closed disjoint regions are independent from each other. See, e.g., Diggle (2003) for details.

distances (due to the clusters associated to the sources) and long distances (due to the decrease of the mean distance). A theoretical derivation of the Rayleigh distribution, for a pure Poissonian field, can be found in Tinebra (2011). A simple indicator of clusterization is the mean value of the MST length. The total length of a MST in a field with a uniformly random distribution of nodes is proportional to \sqrt{AN} (Gilbert 1965) where A is the field area. The mean length for a random-field MST can be written as:

$$\Lambda_m = C\sqrt{\frac{A}{N}} \quad (1)$$

A theoretical upper limit to C equal to $2^{-1/2} \simeq 0.70$ was established by Gilbert (1965), and our Monte Carlo simulations (Campana et al. 2008) consistently found a C value close to 0.65. Thus, if the mean length for a field is quite lower than this value, it can be considered as an indicator of non-random clusterization, i.e. of the presence of sources.

3 MST application to the γ -ray sky

In the practical applications of MST-based cluster extraction to γ -ray sky images, we have to take into account several complications, arising from the presence of large scale structures mainly due to the Milky Way high energy emission. After excluding a belt along the Galactic equator having a latitude width of the order of 15° – 20° , there is still an appreciable decreasing gradient of photon density in the directions of the Galactic poles, even at energies higher than 1 GeV. Moreover, spatial features extending to high latitudes are apparent above and below the Galactic centre and in other parts of the disk.

An important consequence of this inhomogeneous photon density for the MST cluster finding is that the mean edge length Λ_m does not correspond to the *local* one, that is shorter in the high density zones and longer in the low density ones. This implies that when Λ_{cut} is given as a fraction of Λ_m , it is possible that several spurious clusters are found in the high density zone. To reduce this effect one can divide the region in a suitable number of overlapping subregions in which the photon density has only rather small variations: clusters are then selected from the central zone of each subregion, avoiding the boundaries where the clustering can be affected by the discontinuity in the photon field. Another problem arises if a bright source is in one of the subregions: the mean edge length in the subregion could be quite lower than in the others, affecting thus the selection of poorer clusters. These peculiar

subregions require a particular analysis, possibly with different choices of the boundaries.

However, once the MST has been obtained for a photon field, a good strategy for selecting spatial clusters and, among them, those having a high probability to correspond to genuine γ -ray sources, is to apply the following two steps:

- **Primary selection:** here we use only the two parameters N_{cut} and Λ_{cut} (Sect. 2) to select all the clusters having the minimum requirements to be a structure in the field. As will be shown in Sect. 6.2, it is usually applied a rather low N_{cut} , and values of Λ_{cut} in the range 0.6–0.8 in units of Λ_m are shown to minimize the number of spurious clusters: a value of Λ_{cut} closer to unity would increase the probability of selecting clusters due to random fluctuations of the background, while a lower value would reduce the selection only to very dense clusters. When searching for point sources one has to take into account the instrumental angular resolution, and values of Λ_{cut} corresponding to edge lengths larger than the radius of the PSF must be rejected. This can be the case for fields with a low mean photon density. Moreover, to avoid a selection of clusters not matching the expected point source characteristics, a lower threshold value on the cut length should be imposed, corresponding to an angular separation a few tenths of a percent greater than the effective PSF radius.

After the application of this step, usually we obtain a rather long list of clusters for which we compute several quantities, the *cluster parameters*, convenient for the further selection. These parameters, defined in Section 5, give a measure of the compactness of the clusters related to some properties of the field and can be used to take into account the expected properties of the γ -ray source population, such as the angular extension to be compared with the instrumental PSF. Then, a further selection can be performed:

- **Secondary selection:** it is based on the definition of selection thresholds to be applied to the cluster parameters and extracts from the first list those having properties expected for best candidates of “true” point-like sources. The main objective is to maintain in the final list clusters having a high probability to be associated with genuine astrophysical sources and to eliminate those originating from density fluctuations of the cosmic background and residual cosmic rays.

4 Source location accuracy

A good estimate of source positions in the sky is very important for the secondary selection, for the comparison between MST results with those of other methods, and for the association of possible counterparts. The simplest approach is the calculation of the centroid position, i.e. the arithmetic mean of the coordinates of all photons belonging to a selected cluster. Generally, this elementary method gives a good estimate of the source coordinates. In some cases, however, it can fail to provide a satisfactory location for different reasons: *i*) the cluster is in a relatively high background region and its shape can be highly irregular; *ii*) the separation value is not small enough and the cluster extends in a particular direction with a branch well outside the PSF size; *iii*) connection and/or proximity with another cluster, producing an enlarged structure; *iv*) small number of nodes; *v*) sufficient number of nodes but moderate clustering, particularly relevant for sources with soft spectra.

Starting from the first centroid position defined above, one can refine it by means of: *i*) using suitable “weights” in averaging nodes’ coordinates, *ii*) applying a further selection of the nodes to be used in the calculation based on their distance from the first centroid. The method of weighted averages is justified by the energy dependence of the PSF radius, quite smaller at higher than lower energies. Weights, therefore, could be related to this additional information, because high energy photons are expected to have a higher concentration around the ‘true’ source position. Another possibility, which takes into account this property implicitly, is the use of photons’ coordinates to establish the weights. We thus introduced as a weight the q -th power of the distance from any node to the nearest one, $1/\lambda^q$. However, the possible occurrence in a cluster of a couple of events with a very small angular separation between them, but located far from the first centroid, would produce a large difference of their weighted positions with respect to the initial one. This effect was found not negligible even for clusters having a particularly high number of nodes and can be avoided by excluding from the calculation a fraction of nodes at high distance from the centroid.

To establish the best values of q and of the fraction of excluded photons Tinebra (2011) tested the method by analysing the differences of coordinates with respect to a sample of 130 sources from the 1FGL catalogue, selected with different number of photons and cluster parameters, with the exclusion of bright sources for which the centroid estimates are generally very good.

It was found that the most convenient solution, also from a computational time point of view, was to consider only the fraction of 6/7 of the nodes closest to the initial centroid position, together with an exponent $q = 1$ (for more details, see Tinebra 2011). This choice was a trade-off between avoiding the elimination of events in poor clusters (i.e. with $n < 6$) and to select the fraction of nodes close to the first centroid location in the ones with a high event number, which have a high probability of contamination from the surrounding background. An improvement of coordinates for the 80% of sources was obtained, while all the worsenings were smaller than 0.1 degree, well inside the LAT PSF radius⁴, and thus without practical effects for the search of counterparts.

We further verified this method for evaluating the central position of clusters by comparing our MST results, at energies higher than 3 GeV, with the coordinates of a large sample of 400 active galactic nuclei extracted from the 2 year Fermi-LAT AGN Catalog 2LAC (Ackermann et al. 2011) that reports the most likely radio and optical counterparts of 2FGL sources. About 90% of the MST positions have an angular separation smaller than $6'.7$ ($\sim 0°.1$) with respect to the source position. The same fraction of 2FGL positions (estimated by ML) have an angular separation smaller than $4'.7$ ($\sim 0°.08$). On average, the positional accuracy of MST differs with respect to ML by $1'.2$ ($0°.02$), much lower than the PSF size at these energies. We can conclude that our algorithm provides an estimate of the clusters’ centres good enough to search for reliable counterparts.

5 Cluster parameters

In Campana et al. (2008) we defined two quantities useful to evaluate the “goodness” of the clusters after the primary selection: the number of nodes n_k in the k -th cluster and the *clustering degree* $g_k = \Lambda_m/\lambda_{m,k}$, where $\lambda_{m,k}$ is the mean of the edge lengths in the k -th cluster. From a practical point of view, the former parameter increases with the mean flux of the source, while the latter depends on the spectrum, because sources with a small mean separation between nodes usually have a higher fraction of high energy photons. A secondary selection that uses a severe cut on g , particularly in regions of non uniform or high background, would reduce the efficiency for the detection of soft sources even with a relatively high number of nodes. To limit this effect it is useful to consider the quantity

$$M_k = n_k g_k, \quad (2)$$

⁴http://www.slac.stanford.edu/exp/glast/groups/canda/lat_Performance.htm

that combines the number of nodes with their clustering degree and that we named *magnitude* (Massaro et al. 2009b). A cluster with a small number of nodes, but with very short edge lengths, can have a magnitude comparable to that of a richer but not so dense cluster.

It is possible to define other similar parameters. After the separation step, two sets of edges are obtained: one includes all the edges between connected nodes in clusters and the other contains all the edges pertaining to disconnected nodes. This latter set represents the background in the field. One can then compute the mean values of these sets, Λ_m^C and Λ_m^B respectively, and evaluate the corresponding clustering degrees: $g_k^C = \Lambda_m^C / \lambda_{m,k}$ and $g_k^B = \Lambda_m^B / \lambda_{m,k}$. Clearly, in a given field, one has $g_k^B > g_k > g_k^C$, since on average the “background” edges (Λ_m^B) are longer than the “cluster” edges (Λ_m^C). In other words, g_k^B and g_k^C quantify the amount of clustering with respect to the background and other sources, respectively. In fact, g_k^B and g_k^C are useful when comparing clusters detected in different regions (or subregions). For each cluster one can also consider the magnitudes M_k^B and M_k^C , defined in a similar way to M_k , but using the corresponding clustering degrees. In the following applications, we will consider only the magnitude given by Eq. 2 and analyse its statistical meaning.

When the primary selection is performed using a too small value of Λ_{cut} , it is possible that a rich cluster of nodes is divided into some minor structures, while it would be a unique cluster by applying a slightly larger separation value. These *satellite clusters*, usually located in the surroundings of a true bright source, are generally artifacts of the primary selection and must be properly taken into account in the subsequent analysis. For each cluster, we can introduce a new quantity, named the *proximity value* p , equal to the angular distance to the nearest cluster. Thus, clusters with p higher than a few times the PSF radius (e.g. $\sim 1^\circ$ in LAT images at GeV energies) have a high probability to be genuine sources, while $p < 0.5$ can be the indication for a satellite cluster. The spatial structures of all the clusters with small p needs further investigations before taking a final decision on them.

Two other parameters that can provide useful information on the cluster extension are the *cluster radius* R_c and the *median radius* R_m , defined as the radius of the circle centered at the improved centroid of the cluster (see Sect. 4) and which includes all and half of the n_k nodes, respectively. A high value of clustering parameter g_k usually corresponds to small values of these radii, although in a few cases this property is not verified. This can occur when the cluster exhibits an elongated feature in some direction, likely due to some

background pattern. Again, clusters with R_c or R_m values higher than those expected for a radially symmetric structure, typically comparable or lower than the effective radius of the instrumental PSF, should be further investigated to verify whether they can be associated with genuine sources or not.

We found that the magnitude is the most efficient parameter for the secondary selection. In Sect. 6, we will show that by applying a suitable threshold to the M value, the majority of spurious clusters, i.e. not originated by true sources, can be rejected with a limited loss of good ones.

6 MST application to test fields

6.1 Description of the simulated test fields

To verify the capability of the MST method and to devise the criteria for the secondary selection, in order to provide a high efficiency in accepting clusters associated with “true” sources and rejecting the spurious ones, we applied the above procedure to simulated photon fields with properties similar to the LAT γ -ray sky outside the Galactic belt. To work well with the MST a low density field is preferred: in fact, when the mean angular distance between the photons is smaller than the angular precision of the arrival direction, sources can be close to the confusion limit, and the detection efficiency of clustering algorithms is reduced. Low-density fields, characterised by a mean photon separation comparable or greater than the PSF radius (see Sect. 7.1) are obtained by selecting photons with energies greater than a few GeV, which are characterised also by a rather stable and small PSF radius.

We considered a rather broad region covering an extension of $90^\circ \times 25^\circ$ in Galactic coordinates, precisely, $80^\circ < l < 170^\circ$ and $40^\circ < b < 65^\circ$. The 2FGL catalogue (Nolan et al. 2012) reports 57 sources within this region: some of them have soft spectra and only a small number of detected photons above a few GeV. Using the standard tool `gtobssim`⁵ developed by the *Fermi*-LAT collaboration, we simulated a 2-year long observation of the diffuse γ -ray background (Galactic and isotropic, using the `gll_iem_v02` and `isotropic_iem_v02` models) at energies above 3 GeV. This energy, lower than that used in the previous analyses, was chosen in order to slightly increase the photon number and to reduce possible bias in the comparison of our results with those of the 2FGL catalogue for the true LAT sky field (see Sect. 7.1). The instrumental response function

⁵<http://fermi.gsfc.nasa.gov/ssc/data/analysis/scitools/help/gtobssim.txt>

(IRF) P6_V3_DIFFUSE was used, combining “front” and “back” events. The total number of photons generated in this region is 9322. To this photon list, we added 70 simulated sources. For each source, the number of photons was chosen from a probability distribution given by a power-law, with exponent -2 from a minimum value of 4 up to 40 photons, joined to a constant tail up to 240 photons, rather similar to the flux distribution of the sources in 2FGL. Photon numbers of simulated sources vary between 4 and 228, with the distribution shown in Fig. 2, for a total of 1722 photons. Events in each source are spatially distributed with a Gaussian probability function with $\sigma = 0^\circ.2$ centered at its location. This is a rather poor approximation of the LAT instrumental PSF at these energies, but we decided to use this simplified approach because in our analysis we considered only the coordinates of individual photons and not their energy. The photon spatial distribution was the same for all the sources and we were able to directly compare it with the size of clusters found by MST.

Several simulated test fields have been generated, adding the simulated sources to the same diffuse background. The number of photons for each source is the same for all the realizations, but locations are randomly chosen to have different brightness contrast between sources and the surrounding background.

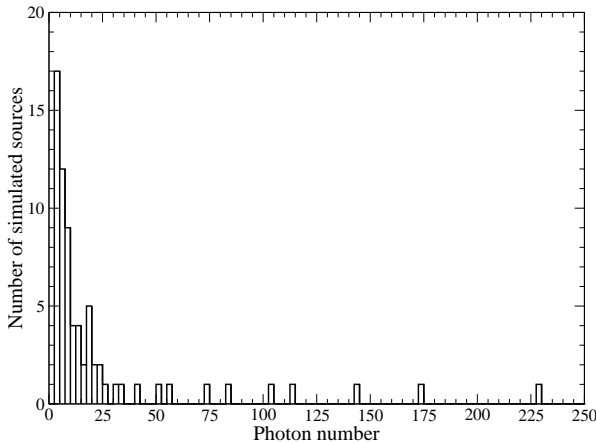


Fig. 2 Distribution of the number of photons in the simulated source set: note the power law shape up to 40 photons and the uniform tail up to ~ 250 photons.

6.2 Test field results

6.2.1 Sensitivity

Considering that the minimum number of photons in the simulated sources is 4, and that some of these

clusters are expected to have one or more background events in the close surroundings, in the primary selection we adopted $N_{\text{cut}} = 3$, while Λ_{cut} was fixed at $0.7 \Lambda_m$. This primary selection produced about 170 clusters in all the simulations. A small increase of Λ_{cut} (e.g. to $0.9 \Lambda_m$) produces a higher number of clusters, because groups of nodes with larger separations between them remain connected. However, the majority of these clusters is characterised by low values of g and photon numbers just above N_{cut} , and many are usually rejected in the secondary selection. Therefore, there is no real advantage to use separation lengths closer to Λ_m . Conversely, values of Λ_{cut} equal or lower than $0.6 \Lambda_m$ actually increase the appearance of satellite clusters and the risk of eliminating true sources with a small number of events or with low clustering parameters. Then the choice of a separation value equal to $0.7 \Lambda_m$ appears to be a satisfactory trade-off in the practical MST application. MST thus finds on average 62.5 ± 3.5 “true” clusters corresponding to about 90% of the 70 simulated sources. The “lost” clusters are mainly composed of 4 and 5 photons: the average number of these is 4.7. This shows that the method is quite sensitive for finding clusters of more than 5 photons. However the number of spurious clusters (i.e., of purely statistical origin) is high: on average 106 ± 1 spurious clusters are generated. For this reason a further selection is necessary.

6.2.2 Spurious cluster rejection

The aim of this secondary selection is to reach the highest rejection of clusters not corresponding to genuine sources together with the lowest elimination of the good ones. Many cluster parameters among those listed in Sect. 5, like R_c , R_m , etc., may be used, but for this purpose we find that n , g and M are the most efficient. We computed for each parameter the normalised cumulative distribution (NCD) for spurious and true sources averaged over the simulated test fields. Fig. 4 shows the NCDs for M , which is found to be the best parameter to reject spurious clusters with the lowest elimination of good ones. The red curve corresponds to the NCD of spurious clusters and the blue one to the NCD of clusters corresponding to true sources. n is a quite good parameter also, but slightly worse than M because it does not take in to account the density of photons. To select the best value of M we also computed the NCD of M for all the sources (both spurious and true, black curve in Fig. 4). It is easy to see that the probability $P(M_{\text{cut}})$ to find true sources with $M > M_{\text{cut}}$ is given by:

$$P(M_{\text{cut}}) = 1 - \frac{N_s[1 - C_s(M_{\text{cut}})]}{N_a[1 - C_a(M_{\text{cut}})]}, \quad (3)$$

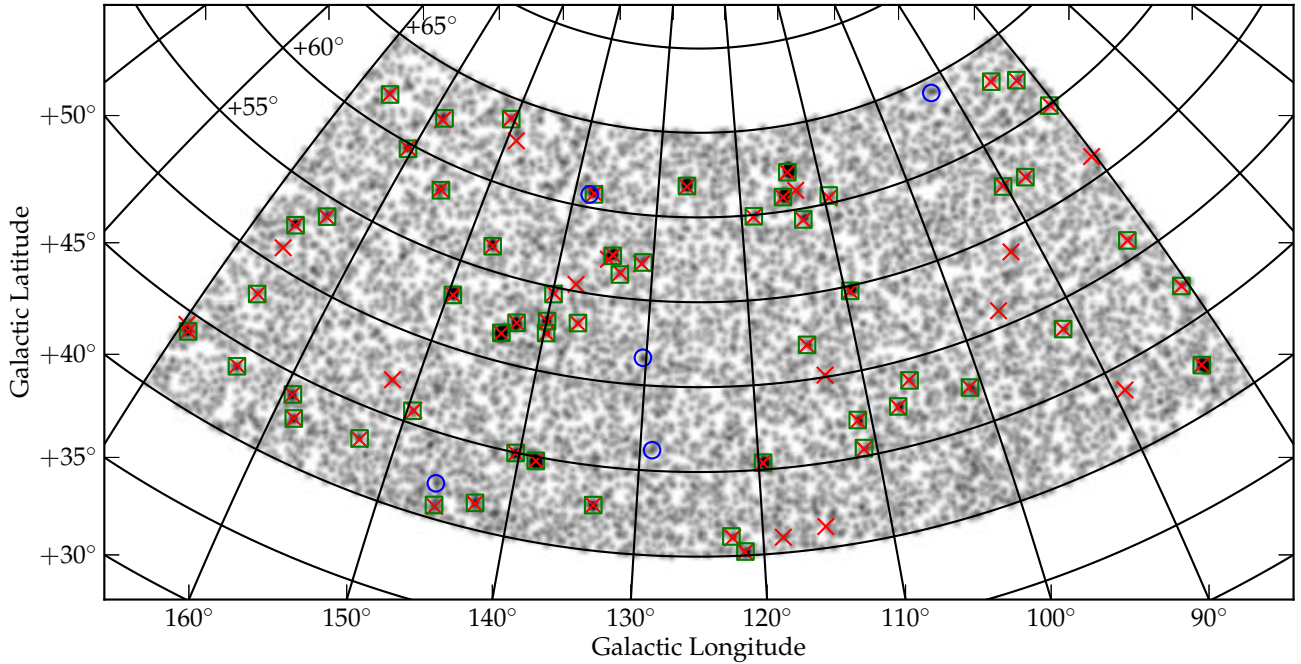


Fig. 3 Aitoff-Hammer projection in Galactic coordinates of one of the simulated 2-year test fields with the additional 70 sources: red crosses mark the original source positions, green squares are the positions of clusters found by MST, blue circles are the spurious detections.

where N_s and N_a are the total numbers of spurious and all sources, respectively, and C_s and C_a are the respective NCDs. For $M = 0$ all the clusters are included and the probability is simply given by the ratio between the number of true clusters $N_t = N_a - N_s$ and the total number of clusters N_a . When the NCD of spurious clusters C_s is close to unity, the probability of finding true sources also approaches unity. In this way it is possible to assign a precise statistical meaning to a selection based on M . In our case, a value of M_{cut} around 15 gives a 90% probability to find true sources.

Applying this cut, the average number of recovered true sources is reduced to 54.0 ± 2.5 , but the average number of spurious ones is reduced to 6.7 ± 0.8 . That is, while the number of selected clusters belonging to a true source is reduced by 14% upon the application of the secondary selection, the “background” of spurious clusters is suppressed by 94%. Observe that for $M > 20$ the probability that a cluster corresponds to a genuine source tends to unity. However, the knowledge of N_s and C_s for real fields can be inferred only on the basis of simulations or statistical considerations.

In Fig. 3 we reported the positions of sources (red crosses) and those of the clusters detected by MST with $\Lambda_{\text{cut}} = 0.7 \Lambda_m$ (green squares) for one simulation. Blue circles mark the positions of spurious clusters, i.e. having the centroid’s coordinates not matching those of the simulated sources. Note that one of them is very close

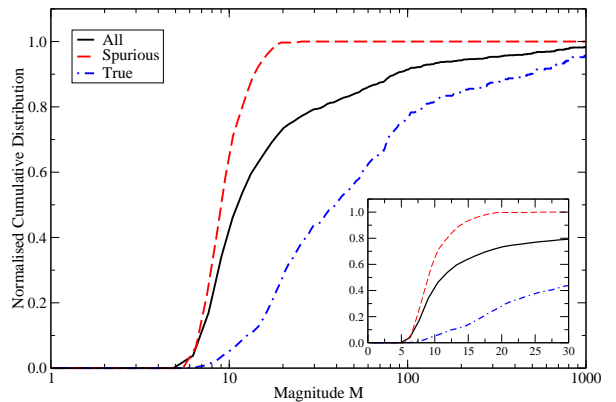


Fig. 4 Normalised cumulative distributions for M on the simulated test fields, for all the sources (true and spurious, black continuous curve), for spurious sources (red dashed line) and true sources (blue dot-dashed line). The range $M = 0-30$ is shown in more detail and in linear coordinates in the inset.

to a true source, and is probably a satellite cluster produced by the fragmentation of the latter.

The cumulative results of the simulations are summarized in Table 1 and shown in Fig. 5, upper panel, which shows the mean fraction of sources found and spurious, as function of the number of generated photons.

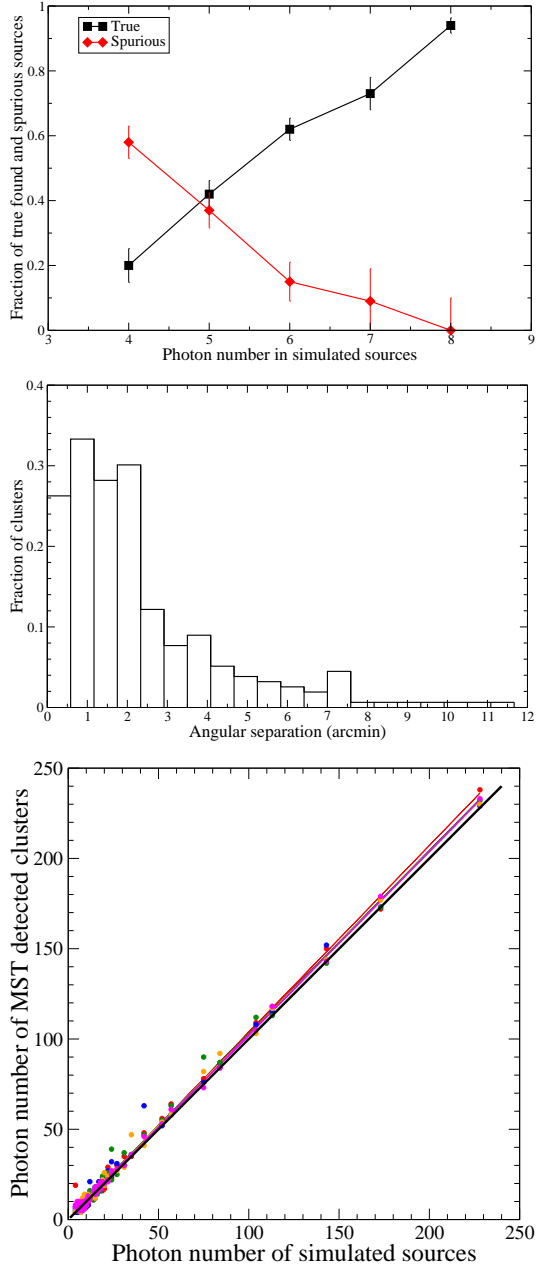


Fig. 5 *Upper panel:* Cumulative results for the MST analysis of the simulated test fields. The fraction of sources found or spurious is plotted, as a function of n . *Central panel:* Histograms of the angular distances between the source locations and the MST centroids of associated clusters. *Lower panel:* Scatter plot of the number of photons of clusters detected by MST against the number of photons for some simulated test fields. The black thick solid line represents the case in which the two numbers are equal.

Table 1 MST results on the simulated test fields. Primary selection parameters are $\Lambda_{\text{cut}} = 0.7 \Lambda_{\text{m}}$ and $N_{\text{cut}} = 3$. For the secondary selection: $M_{\text{cut}} = 15$.

Sources found (w/o secondary select.)	62.5 ± 3.5
Spurious clusters	106 ± 1
Sources found (w/ secondary select.)	54 ± 2.5
Residual spurious clusters	6.7 ± 0.8

6.2.3 Flux and positional accuracy

The accuracy of the weighting method for the evaluation of centroid positions, described in Sect. 4, is confirmed by the histograms of Fig. 5, central panel, where the angular separation of the estimated positions from the correct ones is presented, for all the simulations together. The large majority of sources has distances smaller than $4'$ and only very few cases are found more distant than $6'.5$. Some of the latter ones correspond to pairs of simulated sources located at very small distances, not separated by the adopted MST cut length and joined in a unique cluster. Considering that the 1σ radius of the Gaussian distribution used in the generation of source photons is $12'$ ($0^\circ.2$), our method for estimating the centroid position is confirmed to be accurate enough for a safe positional association.

Fig. 5, lower panel, shows the scatter plot of the number of photons in the clusters detected in tests against the original number of simulated events. The results are very similar in all the simulations and differences are of a few events only. MST numbers for rich clusters are slightly in excess with respect to the original ones: for the richest clusters the mean excess is about 2%. The MST method is thus able to correctly recover the right event number of true sources. There are, however, a few cases with a rather high discrepancy. Again, they are related to very close pairs of sources, not resolved by the cut length. These cases are a few percent in each simulation and can be identified only from a different analysis.

Note that large scale inhomogeneities in the spatial distribution of photons within the entire field are not present (Fig. 3) and, therefore, it was not necessary to consider smaller subregions for the MST analysis.

We did not find that a threshold on the median radius R_{m} and the proximity value p are directly useful in the secondary selection, but provide more information on the extension and near environment of clusters. In particular, we verified that the dispersion of R_{m} values depends on the photon number n_k : for relatively high photon numbers, $n_k > 15$, R_{m} converges to the width of the Gaussian profile of simulated sources (or to the PDF effective radius in true data fields), while

for clusters with n_k lower than this value, it is highly dispersed and values up to ~ 2.5 times the expected ones are found for both genuine or spurious clusters. Therefore, it is not efficient in the rejection of the latter ones originating from background fluctuations, but can be a useful indicator for detecting anomalous extension in rich clusters possibly related to the occurrence of unresolved close pairs.

7 PGW analysis and significance of the detection

The same simulated test fields were also analysed using the PGW algorithm to compare its results with those obtained by MST. This method applies a 2-dimensional Mexican-hat wavelet transform to a γ -ray image, structured as a set of pixels whose intensity is the number of events within each of them. Basically, it employs the algorithm described by Damiani et al. (1997) that provides for each detected source, in addition to coordinates and intensity, also an estimate of its statistical significance measured in terms of the number of standard deviations above the background level, usually indicated as *k-significance* (hereafter k_{PGW}). This method was already applied to simulated LAT images (Ciprini et al. 2007) and was also used in the preparation of the 1FGL (Abdo et al. 2010) and 2FGL catalogues (Nolan et al. 2012). PGW results confirm all the “rich” clusters found by MST, whereas several weak clusters are undetected together with a small number of non-genuine sources. Typically, about 80% of detections are common to both methods, and MST appears to be slightly more efficient in the detection of genuine clusters with a small number of photons.

7.1 Statistical significance of MST source detection

In Campana et al. (2008) we studied the probability distributions of g and n in uniform random fields generated by a Monte Carlo extraction of nodes. A straightforward application of these results to the real sky, however, is not practical and does not always give good estimates of the chance detection probability, because of the non-uniform γ -ray background and the deviation from a purely random distribution due to the occurrence of strong sources.

We searched for a simple and reliable estimator of the statistical significance of individual sources by comparing the MST cluster parameters with the k_{PGW} values obtained by means of PGW in the simulated fields. In principle, one can expect that the magnitude M of a cluster can be such an estimator because it depends on

the number of photons and therefore can be correlated with the PGW significance. The plot of $\text{Log } k_{\text{PGW}}$ vs $\text{Log } M$ shows, in fact, a very high linear correlation and a simple power law best fit gives exponents for M close to 0.5, within a few percent. We then assumed this value as the correct one and plotted the values of k_{PGW} vs \sqrt{M} for all the simulated fields (Fig. 6, left panel). The correlation between these two quantities is very high, despite a small number of points lying at a rather large distance from a linear trend. A simple relation able to describe well the data of all the simulations is

$$k_{\text{PGW}} = S\sqrt{M} \quad (4)$$

with $S = 0.8$. This relation can be considered as a simple practical rule for evaluating the statistical significance of a cluster detection by MST. Note that, according to this criterion, the requirement that a cluster would have at least a significance $k_{\text{PGW}} = 3$ would imply a threshold value for M equal to 14, that is practically coincident to the value we found to optimize the ratio of number of lost sources to that of spurious ones.

8 Analysis of the *Fermi*-LAT field

We verified Eq. 4 applying the two methods to the true 2-years LAT field used for the 2FGL catalog (Nolan et al. 2012), covering the same region of the simulated fields and selecting photons in the energy range 3–100 GeV and detected between 2008 August 5 and 2010 August 5. This field is well suited for a cluster analysis because the density gradient of photons toward low Galactic latitudes is mild: the mean angular separation between photon pairs changes from about $0^\circ.25$ close to the high b boundary to about $0^\circ.2$ close to the lower one. It is therefore always comparable with the radius of the instrumental PSF in this energy range. LAT events were selected in a rectangular box corresponding to the test field Galactic coordinates, and we applied the standard cut on the zenith angle ($<100^\circ$) and on the rocking angle ($<52^\circ$) to limit contamination from Earth limb γ -rays. The 2FGL catalogue reports 57 sources with $TS > 25$ in the 100 MeV–100 GeV energy range inside the true LAT test field. Only 38 of these are detected above 3 GeV, and 12 of this latter group have TS lower than 25 in this energy range. The application of MST with the criteria for secondary selection given above ($M > 15$) finds 39 significant clusters associated with the 2FGL sources: 37 correspond to 2FGL sources detected above 3 GeV and the remaining 2 correspond to 2FGL sources detected only in lower energy bands; the only 2FGL source with a measured flux in

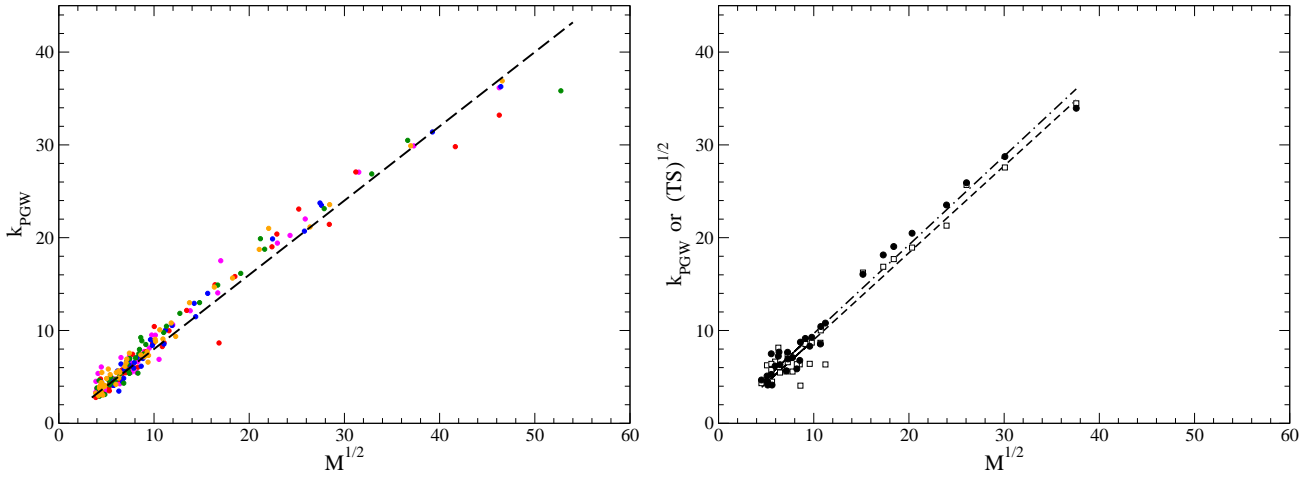


Fig. 6 *Left panel:* The relation between the PGW k -significance and the square root of the magnitude M in the simulated test fields. The thick dashed line represents the law $s = 0.8\sqrt{M}$. *Right panel:* the magnitude-significance relation for the 2 year 3–10 GeV true LAT field. Filled circles correspond to the MST and PGW significance plot, while open squares correspond to relation of \sqrt{M} with \sqrt{TS} for the 3–10 GeV band reported in the 2FGL catalogue. The dashed and the dot-dashed lines represent the best fits for \sqrt{M} vs. k_{PGW} and \sqrt{M} vs. \sqrt{TS} relations, respectively.

the 3–10 GeV energy band and not detected by MST has the quite low $TS = 9.6$ in this band.

Among the sources detected by the two methods, we selected a subset of 32 sources having $k_{\text{PGW}} > 4$ and plotted their k -significance vs \sqrt{M} (Fig. 6, right panel): again a high linear correlation resulted. A similar correlation is also found with the ML significance \sqrt{TS} in the 3–10 GeV band, extracted from the 2FGL catalogue. In both cases, the best fit values of S were very close to unity: 0.94 and 0.96, respectively. Note that the residuals of data points with respect to best fit lines are higher for the 2FGL \sqrt{TS} set than for k_{PGW} , particularly for sources with $\sqrt{M} < 15$ and, therefore, with signal-to-noise ratios that are not very high. This effect can be due to the fact that \sqrt{TS} in the catalogue were evaluated in an energy band narrower than the one used by us, and therefore photon numbers of some individual sources can be lesser than ours.

An intuitive explanation of Eq. 4 can be based on the quasi-Poissonian spatial distribution of photons in the field. In this case, in fact, one can reasonably associate with a cluster of n_k photons, (which is one of the two factors in the definition of M) a standard deviation equal to $\sqrt{n_k}$. Considering that the range of the clustering degree g is generally limited from 2.5 to ~ 10 , with the large majority of values lower than 6 (in our simulations the mean values of g were always close to 4.2 with a rms value of 1.5), the additional variance due to this quantity is not large. Thus a linear relation between k_{PGW} and \sqrt{M} would be expected. We verified in our simulations also the occurrence of a high linear correlation between $\sqrt{n_k}$ and k_{PGW} . Neverthe-

less the use of the magnitude, instead of the number of photons, appears more convenient for the following reasons: *i*) the secondary selection based on M , that takes implicitly into account the cluster density, is more efficient in selecting the poorest clusters than a procedure based on n_k ; *ii*) the parameters of the linear regression are found more stable when the different fitting intervals in $\sqrt{n_k}$ or \sqrt{M} are considered. We do not have a complete theoretical explanation for this fitting stability and for computing the expected value of S . Anyway, our results suggest the following practical approach: having obtained a list of common clusters with MST and another method, one can select a sample of high significance sources in the latter set to be used for evaluating the best S value.

9 New candidate γ -ray sources

In addition to clusters associated with already known γ -ray sources, our MST analysis of the LAT test field provided a number of clusters having rather high values of M , and therefore a high confidence to be not spurious. Nine clusters with $M > 19$, 6 of them with $n > 8$, are reported in Table 2; these threshold values did not give spurious detections in the simulated field analysis (Sect. 6.2). They are divided into two groups, based on their number n of photons ($n \geq 9$ or $n < 9$), the former ones are expected to have a higher confidence to be genuine.

We also searched for possible counterparts to be associated with these clusters to make their detections more

robust as genuine γ -ray emitters. We found interesting positional correspondences within an angular distance of $0^\circ.2$ for four of them with BL Lac objects from the *Roma-BZCAT* (Massaro et al. 2009a, 2011). Considering that this catalogue reports 115 BL Lac objects and candidates within the entire considered LAT field, which covers about 1360 square degrees, their mean density is about 0.085 sources deg^{-2} . The resulting chance probability to find one BL Lac object within a circle with a radius of $0^\circ.2$ is $\sim 1.1 \times 10^{-2}$. Thus, we obtain a chance probability for 4 associations out of these 9 trials of the order of 3×10^{-6} . It appears very unlikely that these associations would be found if all clusters were spurious. Note that we did not find possible counterparts classified as flat spectrum radio quasars, in agreement with the expectation that they generally have soft γ -ray spectra and therefore a low photon flux above 3 GeV (Ackermann et al. 2011). The possibility to find radio sources within the same angular radius is, of course, much higher, but the majority of them are generally rather weak and without optical counterparts. Only in two cases we found bright radio sources (also reported in Table 2) but they do not exhibit definitive blazar characteristics and their association with γ -ray emission appears unlikely.

A further interesting finding is that four clusters with $n > 8$ have g values lower than 2.5, and two of them slightly lower than 2, indicating that their “clumpiness” is low. Among the 37 clusters associated with 2FGL, 18 have $g < 3$, and 4 have $g < 2.5$. Some of the newly detected features could be associated with extended structures or with pairs of sources having a small angular separation, comparable to the instrumental resolution, and therefore they can be missed by algorithms based on the matching with the PSF shape. A more detailed analysis over regions having a size of 10° and centered at the cluster likely associated with BZB J1123+7230 separates it into two smaller groups: one having 6 photons ($M = 11.99$) closer to the blazar position, and the other with 8 photons ($M = 22.83$) and having coordinates $\text{RA} = 170^\circ.48$, $\text{Dec} = 72^\circ.41$ without a known possible counterpart. Note also that the latter cluster is found at energies higher than 6 GeV, with 6 photons and $M = 18.2$. Applying the shorter separation length $\Lambda_{\text{cut}} = 0.5 \Lambda_{\text{m}}$ the two clusters are split again, one of them with $n = 5$ and $M = 24.0$. A similar analysis for the cluster close to BZB J1327+6458, which has a rather low g value, gives a detection above 6 GeV with 7 photons and $M = 16.8$, but a centroid position slightly more distant from the possible BZB counterpart, and about at the same separation from the radio source NVSS J074638+520042, of which no optical counterpart is known. We cannot exclude, therefore, the occur-

rence either of a possible confusion or of a spurious association. The other two associations with BZB sources reported in Table 3, appear to be positionally more robust, in particular the one with BZB J1237+6258, that has a high g although with only 6 photons. This source is located very close to the southern boundary of the field, a circumstance that can affect the construction of the MST; however, a test for the existence of this cluster in a surrounding region 10° size around it confirmed its detection. Again, the analysis of the cluster associated with BZB J1404+6554 at energies above 6 GeV confirms a detection with 7 photons and $g = 2.82$. Finally, we note that only the cluster at $\text{RA} = 207^\circ.32$, $\text{Dec} = 71^\circ.53$, for which no possible counterpart has been found, does not survive the more severe cut. Photon maps of these four clusters are given in Fig. 7.

We also searched for these clusters with the PGW algorithm and the standard ML (ML Abdo et al. 2010) analysis. The former method finds only three detections with a significance in the range between 2.5 and 3 standard deviations. In Table 2, the value of the Test Statistic (TS) for each new MST source candidate was derived applying the binned likelihood method implemented in the standard LAT Science Tools⁶ (version v9r28p0). We analyzed data collected, in the 3 GeV–300 GeV energy range, from 2008 August 5 to 2011 August 5. For this analysis, only events belonging to the Pass 7 “Source” class and located in a circular region of interest (ROI) of 10° radius, centered at the position of the MST candidate source were selected. We applied the standard cuts on the zenith angle ($< 100^\circ$) and on the rocking angle ($< 52^\circ$). The ROI model used by the binned likelihood method includes all point sources from the 2FGL catalog (Nolan et al. 2012) located within 15° of the MST candidate source. Sources located within a 2° radius centered on the MST source position had all spectral parameters left free to vary during the fitting. The MST candidate was modeled as a power law with both normalisation and spectral index free to vary. We used IRF version P7SOURCE_V6⁷. The diffuse Galactic and isotropic components were modeled with the same ones used for generation of 2FGL (`gal_2yearp7v6_v0` and `iso_p7v6source` files⁸). The normalisations of the components comprising the total background model were allowed to vary freely. For all the MST candidate sources reported in Table 2 we found $TS < 25$ (with 2 degrees of freedom, spectral index and normalisation, $TS = 25$ roughly corresponds to a 4.6σ detection significance).

⁶<http://fermi.gsfc.nasa.gov/ssc/data/analysis/scitools/overview.html>

⁷http://www.slac.stanford.edu/exp/glast/groups/canda/lat_Performance.htm

⁸<http://fermi.gsfc.nasa.gov/ssc/data/access/lat/BackgroundModels.html>

Table 2 Coordinates and main properties of MST clusters detected in the 2 year LAT test field and not associated with sources in the 2FGL catalogues. Maximum likelihood significance is reported only when $TS > 9$. Celestial coordinates are J2000.

RA deg	Dec deg	l deg	b deg	n	g	M	PGW det.	TS	ang. dist. arcmin	Possible counterparts
170.49	72.40	132.00	43.11	14	2.652	37.128	yes	24.3	10	BZB J1123+7230 (¹)
179.00	61.61	134.18	54.29	9	2.427	21.843	no	11.6	—	—
201.89	64.84	116.73	51.85	10	1.941	19.410	yes	—	8	BZB J1327+6458 (¹)
207.32	71.53	116.52	44.87	10	1.956	19.560	no	—	—	—
210.97	65.91	111.65	49.60	11	2.141	23.551	yes	—	6	BZB J1404+6554; 4C 66.14 (²)
237.64	60.34	93.32	45.14	9	2.746	24.714	no	15.6	—	—
142.46	66.38	146.76	40.17	8	2.408	19.264	no	—	6	TXS 0925+665 (³)
158.13	69.19	139.08	43.32	7	2.998	20.986	no	—	—	—
189.36	62.94	125.65	54.12	6	3.338	20.028	no	12.6	3	BZB J1237+6258

1: possible pair of clusters.

2: bright compact and steep spectrum source at a distance of $3'.47$ from the cluster centroid.

3: steep spectrum radio source with a bright core and two possible lobes of much weaker brightness.

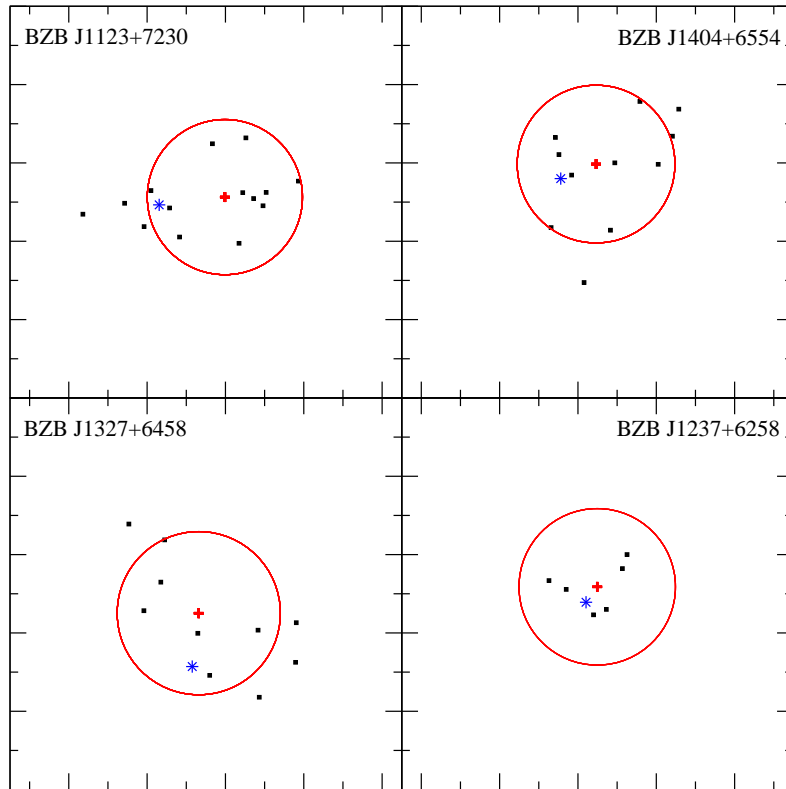


Fig. 7 Photon maps (between 3 and 100 GeV) of four new detected clusters having possible BL Lac counterparts. Each panel is $1^\circ \times 1^\circ$ wide and oriented with the Galactic coordinates. Photon longitude distances from the centroid have been scaled by the cosine of the latitude. Red crosses mark the centroid positions and the circles delimit regions having a radius of $0^\circ.2$. Blue stars mark the coordinates of possible BL Lac counterparts: BZB J1123+7230 (top-left), BZB J1327+6458 (bottom-left), BZB J1404+6554 (top-right), BZB J1237+6258 (bottom-right).

10 Conclusions

The application of MST to true and simulated LAT images confirms the validity of this method for searching γ -ray sources, especially for weak ones.

We defined and investigated the properties of the parameter M , or magnitude, defined as the product of the clustering degree and the number of nodes in a given tree, that was found to be very useful in the selection of statistically robust clusters. An application to simulated and true LAT fields, in comparison with the PGW method, has shown that \sqrt{M} gives also a quite good estimate of the statistical significance of a source. Therefore, a secondary selection based simply on a threshold on M close to 15 would reject the large majority of spurious (low significance) clusters. A few other spurious sources can be eliminated by further selections based on the clustering degree g . For a more complete definition of source candidates, it is useful to consider other parameters. The proximity value, i.e. the angular separation to the closest cluster, helps in extracting possible satellite clusters surrounding intense sources and possible extended structures. The cluster and median radii can also provide additional information on that, in particular for the richest clusters.

Our simulated photon fields — satisfying *only* the conditions to have a rather uniform density with average photon angular distances comparable with the LAT PSF — show that sources with a number of photons higher than 6 are expected to have a very high probability to be detected.

The probability of finding a spurious cluster, i.e. not corresponding to a genuine source, increases for smaller numbers of events, but for $4 \leq n \leq 6$ events this probability is of the order of 15%–58% (Figure 5). Therefore, one can reasonably expect that some of them could be found to be actually associated with counterparts at different frequencies. On the other hand, for $n \geq 7$ the probability to find a spurious cluster is lower than 10%.

The application of MST — with the criteria for secondary selection given above — to the true LAT test field shows that the method is rather sensitive to find sources that have quite low statistical significance (TS) according to the ML analysis. Moreover MST detects some clusters that appear to be statistically significant according to the method itself, but show a low or no significance according to other methods (PGW and ML). Some of these clusters show plausible associations with possible counterparts, mainly with BL Lac objects.

The particular advantage in using MST for γ -ray source detection is that its cluster selection is based on the requirement that photon separations must be shorter than a given threshold, and does not directly

depend on the density contrast over sampling size regions. It is therefore well suited to find clusters with a low photon number but high density. Moreover, because it works directly on photon coordinates and does not use pixellated images, it is independent of the actual PSF shape and is able to detect paired clusters that could be missed by other methods.

The limitation of our MST algorithm is that it appears, at the moment, well suited to analyze fields without large gradients in the photon distribution and where the mean photon separation is comparable to the PSF radius. Source detection in fields with a high density of photons, in which the mean angular distance between them is much less than that the instrumental PSF size, and also in fields with large inhomogeneities on different angular scales, is generally a thorny problem for non-local algorithms. In these conditions one can expect that the number of spurious clusters and the fragmentation of strong sources in several clusters make the proximity analysis difficult. For long separation distances, in several cases extended structures not compatible with a point source are selected. Improved selection criteria should then be developed in this case, possibly to be adapted for the search of particular classes of γ -ray sources.

In conclusion, our analysis gives strong indications that the MST algorithm is a very good tool to identify small clusters, corresponding to faint sources (which can be associated with sources of low brightness, thus gaining more information on the population of low luminosity blazars and other AGNs). In general, the clusters selected by MST should be further analyzed with other methods able to evaluate the flux and the spectrum of the sources. MST, also considering its limitations and advantages, is able to quickly provide a list of seed sources to be tested with ML, that can contain additional information (e.g. on cluster compactness, as given by g and M) with respect to other cluster finding algorithms.

It should be emphasized that the computation of the MST directly provides information on the mean angular distance between the nodes in the individual clusters and its ratio to that of the field. Consequently, the M -based selection can be easily applied to extract clusters having a high probability to be genuine sources without performing other assessments on the local background properties.

The computational time issue is unimportant for our applications to source detection in gamma-ray images. On the basis of our practical work, typical computation time in fields containing a number of photons of the or-

der of 50,000 or more is actually fast enough⁹ and even if it would be longer, this will not be a problem. MST analysis, in fact, is not run in real time during the observations, where a fast result can be necessary, but on off-line archival data accumulated in many months or years of observations. The secondary selection analysis is more time consuming. However, this direct study of the cluster structure is useful to understand the nature of peculiar clusters, such those having a large number N of photons but a low clustering degree.

As a final note, we would like to stress that astrophysical applications of our developments of the MST method are not limited to γ -ray astronomy, but can be easily extended to other research fields where the problem is to search for clustered structures against a background with a random spatial distribution, like in the case of finding star or galaxy groups and clusters or other clumped structures.

Acknowledgments

We are grateful to the referee, Maria Concetta Maccarone, whose helpful comments greatly improved the quality of the text, and to Toby Burnett, Seth Digel and Andrea Tramacere for useful discussions. This research has been partially supported by a grant from Università di Roma “La Sapienza”. The *Fermi*-LAT Collaboration acknowledges generous ongoing support from a number of agencies and institutes that have supported both the development and the operation of the LAT as well as scientific data analysis. These include the National Aeronautics and Space Administration and the Department of Energy in the United States, the Commissariat à l’Energie Atomique and the Centre National de la Recherche Scientifique/Institut National de Physique Nucléaire et de Physique des Particules in France, the Agenzia Spaziale Italiana and the Istituto Nazionale di Fisica Nucleare in Italy, the Ministry of Education, Culture, Sports, Science and Technology (MEXT), High Energy Accelerator Research Organization (KEK) and Japan Aerospace Exploration Agency (JAXA) in Japan, and the K. A. Wallenberg Foundation, the Swedish Research Council and the Swedish National Space Board in Sweden. Additional support for science analysis during the operations phase is gratefully acknowledged from the Istituto Nazionale di Astrofisica in Italy and the Centre National d’Études Spatiales in France.

⁹As an example, for a field containing 50,000 photons, the computational time is shorter than 20 seconds on a 2.2 GHz Intel Core i5 laptop with 4 GB RAM. The secondary selection algorithms account for more than 90% of the overall running time.

References

- Abdo, A.A., Ackermann, M., Ajello, M., Allafort, A., Antolini, E., Atwood, W.B., Axelsson, M., Baldini, L., Ballet, J., Barbiellini, G., et al.: *Astrophys. J. Suppl. Ser.* **188**, 405 (2010)
- Ackermann, M., Ajello, M., Allafort, A., Antolini, E., Atwood, W.B., Axelsson, M., Baldini, L., Ballet, J., Barbiellini, G., Bastieri, D., et al.: *Astrophys. J.* **743**, 171 (2011)
- Barrow, J.D., Bhavsar, S.P., Sonoda, D.H.: *Mon. Not. R. Astron. Soc.* **216**, 17 (1985)
- Bhavsar, S.P., Ling, E.N.: *Astrophys. J. Lett.* **331**, 63 (1988a)
- Bhavsar, S.P., Ling, E.N.: *Publ. Astron. Soc. Pac.* **100**, 1314 (1988b)
- Buccheri, R., Maccarone, M.C., Sacco, B., Di Gesù, V.: *Astron. Astrophys.* **201**, 194 (1988)
- Campana, R., Massaro, E., Gasparrini, D., Cutini, S., Tramacere, A.: *Mon. Not. R. Astron. Soc.* **383**, 1166 (2008)
- Ciprini, S., Tosti, G., Marcucci, F., Cecchi, C., Discepoli, G., Bonamente, E., Germani, S., Impiombato, D., Lubrano, P., Pepe, M.: In: Ritz, S., Michelson, P., Meehan, C.A. (eds.) *The First GLAST Symposium*. American Institute of Physics Conference Series, vol. 921, p. 546 (2007)
- Damiani, F., Maggio, A., Micela, G., Sciortino, S.: *Astrophys. J.* **483**, 370 (1997)
- De Biase, G.A., Di Gesù, V., B., S.: *Pattern Recognition Letters* **4**, 39 (1986)
- Di Gesù, V., Maccarone, M.C.: *Pattern Recognition* **19**, 63 (1986)
- Di Gesù, V., Sacco, B.: *Pattern Recognition* **16**, 525 (1983)
- Diggle, P.J.: *Statistical Analysis of Spatial Point Patterns*, 2nd edn. Arnold Publishers, London (2003)
- Gilbert, E.N.: *Journ. Soc. Ind. Appl. Math.* **13**, 376 (1965)
- Harnden, F.R. Jr., Fabricant, D.G., Harris, D.E., Schwarz, J.: *SAO Special Report* **393** (1984)
- Koenig, X.P., Allen, L.E., Gutermuth, R.A., Hora, J.L., Brunt, C.M., Muzerolle, J.: *Astrophys. J.* **688**, 1142 (2008)
- Krzewina, L.G., Saslaw, W.C.: *Mon. Not. R. Astron. Soc.* **278**, 869 (1996)
- Maccarone, M.C., Buccheri, R., Di Gesù, V.: In: Di Gesù, V., Scarsi, L., Crane, P., Friedman, J.H., Levialdi, S. (eds.) *Data Analysis in Astronomy II*, p. 97. Plenum Press, New York (1986)
- Massaro, E., Giommi, P., Leto, C., Marchegiani, P., Maselli, A., Perri, M., Piranomonte, S., Sclavi, S.: *Astron. Astrophys.* **495**, 691 (2009a)
- Massaro, E., Tinebra, F., Campana, R., Tosti, G.: *ArXiv e-prints* (2009b)
- Massaro, E., Giommi, P., Leto, C., Marchegiani, P., et al.: *Multifrequency Catalogue of Blazars*, 3rd edn. Aracne, Rome (2011)
- Mattox, J.R., Bertsch, D.L., Chiang, J., Dingus, B.L., Digel, S.W., Esposito, J.A., Fierro, J.M., Hartman, R.C., Hunter, S.D., Kanbach, G., Kniffen, D.A., Lin, Y.C., Macomb, D.J., Mayer-Hasselwander, H.A., Michelson, P.F., von Montigny, C., Mukherjee, R., Nolan, P.L., Ramana-murthy, P.V., Schneid, E., Sreekumar, P., Thompson, D.J., Willis, T.D.: *Astrophys. J.* **461**, 396 (1996)
- Nolan, P.L., Abdo, A.A., Ackermann, M., Ajello, M., Allafort, A., Antolini, E., Atwood, W.B., Axelsson, M., Baldini, L., Ballet, J., et al.: *Astrophys. J. Suppl. Ser.* **199**, 31 (2012)
- Plionis, M., Valdarnini, R., Jing, Y.-P.: *Astrophys. J.* **398**, 12 (1992)
- Prim, R.C.: *Bell System Tech. J.* **36**, 1389 (1957)
- Schmeja, S.: *Astronomische Nachrichten* **332**, 172 (2011)
- Schmitt, J., Starck, J.-L., Casandjian, J.-M., Fadili, J., Grenier, I.: *ArXiv e-prints* (2012)
- Starck, J.-L., Murtagh, F., Bijaoui, A.: In: Shaw, R.A., Payne, H.E., Hayes, J.J.E. (eds.) *Astronomical Data Analysis Software and Systems IV*. Astronomical Society of the Pacific Conference Series, vol. 77, p. 279 (1995)
- Tegmark, M., de Oliveira-Costa, A.: *Astrophys. J. Lett.* **500**, 83 (1998)
- Tinebra, F. PhD thesis, University of Roma La Sapienza, Rome (2011)
- Tramacere, A., Vecchio, C.: *Astron. Astrophys.* **549**, 138 (2013)
- Zahn, C.T.: *IEEE Trans. on Computers* **C20**, 68 (1971)